A theoretical study of the (2*1) reconstruction of Si(100): application to surface-induced core level shifts

1992 J. Phys.: Condens. Matter 4 5061

(http://iopscience.iop.org/0953-8984/4/22/006)

J. Phys.: Condens. Matter 4 (1992) 5061–5076. Printed in the UK

A theoretical study of the (2 × 1) reconstruction of Si(100): application to surface-induced core level shifts

T Vinchon†, D Spanjaard‡ and M C Desjonquères†

† CEA, CEN Saclay, DSM, DRECAM, SRSIM, Bâtiment 462, 91191 Gif-sur-Yvette Cédex, France

‡ Université de Paris-Sud, Laboratoire de Physique des Solides, Bâtiment 510, 91405 Orsay Cédex, France

Received 9 December 1991, in final form 2 March 1992

Abstract. The tight-binding method is used to study the (2 × 1) reconstruction of the Si(100) surface. The laws of variation with interatomic distance of the Slater–Koster parameters and of the pairwise repulsion energy are defined in order to give a good description of the electronic band structure and of the elastic properties of bulk silicon. The necessity of taking into account, during the total energy minimization, the surface-induced atomic level shifts is emphasized. The dimer bond length is shown to be in good agreement with experimental values. Then, the atomic level shifts are related to the surface-induced core level shifts. A new interpretation of core level photoemission spectra, consistent with a weak asymmetry of the dimers, is finally proposed.

1. Introduction

If the explanation of the (2 × 1) reconstruction of Si(100) by the formation of dimers is now commonly accepted, a controversy still remains on a possible asymmetry of these dimers. The calculations carried out in the symmetric dimer geometry [1] lead to two overlapping dangling-bond bands giving a metallic character to the surface, in apparent contradiction with angle-resolved ultraviolet photoemission spectroscopy (ARUPS) experiments in which a surface band gap is observed. In order to solve this contradiction, Chadi [2] suggested that the dimers were buckled. This buckling increases the energy separation between the two bands associated with dangling-bond surface states, producing an absolute gap between them. Since this calculation of Chadi, most theoretical work has confirmed this asymmetry even though Wolfgarten *et al* [3] observed, in their *ab initio* calculation, the disappearance of the gap between surface states that they attributed to an artifact of local density approximation (LDA) calculations. However, some computations have led to the opposite conclusion. For example, Pandey [4] found that the tilting of the dimer was not energetically favoured. Moreover, he argued that a missing dimer defect could substantially decrease the surface energy. Furthermore, using a very simple model, Artacho and Yndurain [5] proposed that an antiferromagnetic arrangement of the spins within the dimer could lower the symmetric configuration energy and split the two surface state bands.

From the experimental point of view, several techniques are available but lead to contrasting conclusions. The low-energy [6] and medium-energy ion scattering [7] experiments support the existence of dimers but are unable to distinguish between

0953-8984/92/225061+16$04.50

symmetric and asymmetric dimers. The scanning tunnelling microscope (STM) images [8] were first interpreted as due to a surface consisting mainly of symmetric dimers, the asymmetric dimers being visible near the defects. Then, it was argued [9] that the symmetric dimer appearing on the STM images may actually be the time-averaged position of asymmetric dimers that are rapidly switching between the two possible buckling directions. Finally, very recent experiments [10] have shown that the same dimer may appear symmetric or asymmetric according to the sign of the bias voltage. It has been claimed that this difference in the images may be due to the interaction of the electric field of the STM with the dipole arising from the charge transfer between the up and down atom. This forces the dimer to be symmetric when the tip is negative with respect to the up atom and enhance the buckling when the tip is positive. However, another contribution to this effect may come from the different occupation of orbitals above or below the Fermi level when the dimer is tilted.

Although most ARUPS data are consistent with the asymmetric dimer model, the polarization-dependent ARUPS study of Johansson *et al* [11] indicates a mirror symmetry along the [1,1,0] and [−1,1,0] directions in the surface Brillouin zone in agreement with the symmetric dimer model. Let us note, however, that ARUPS probes excited states whereas the calculations are performed for the ground state. Finally, many core level photoemission spectroscopy experiments [12–18] have been carried out on Si(100) (2 × 1). They have led to different results not only on the number of surface components of the spectrum but also on the assignment of the different components to given atoms.

Moreover, low-energy electron diffraction (LEED) [19, 20] and ion scattering [6] experiments give a dimer bond length significantly larger than those obtained in most calculations. This suggests that the elastic properties of silicon are not well reproduced in the calculations and, thus, it is advisable to check, before any surface calculation, that the calculated bulk modulus is close to the experimental one.

In this work, we present a tight-binding study of the (2 × 1) reconstruction of Si(100) with particular emphasis on the interpretation of core level spectra. In section 2, we first derive a tight-binding Hamiltonian, which, in the bulk, coincides with the Hamiltonian of Pandey and Phillips [21] and, thus, gives a good description of the valence bulk band structure. Then, we check that it leads to a bulk modulus that agrees with experiment. In section 3, we discuss the modifications of the tight-binding formalism for surfaces and, in particular, the shifts of atomic levels in the vicinity of the surface. Then, we present our results on the (2 × 1) reconstruction of Si(100). In section 4, we relate the atomic level shifts to the data of surface core level spectroscopy and present a new interpretation of these experiments.

2. Parametrization of the total energy in a tight-binding model

In the tight-binding approximation, the total energy E_{tot} is written as the sum of two contributions: an attractive term, E_{band}, and a repulsive energy, E_{rep}. The repulsive energy ensures the stability of the crystal. It is assumed to be a pairwise function of the bond lengths.

The band term is obtained from the energy levels, which are found by diagonalizing the tight-binding Hamiltonian:

$$H = \sum_{i,\lambda} \epsilon_\lambda^i |i,\lambda\rangle\langle i,\lambda| + \sum_{i,j}^{\lambda,\lambda'} \beta_{ij}^{\lambda\lambda'} |i,\lambda\rangle\langle j,\lambda'|. \tag{1}$$

The atomic orbitals $|i,\lambda\rangle$ ($\lambda = s, p_x, p_y, p_z$) centred at all sites i are assumed to be orthogonal. The quantities ϵ_λ^i and $\beta_{ij}^{\lambda\lambda'}$ are, respectively, the atomic level of orbital λ at site i and the hopping integral between the orbital λ at site i and the orbital λ' at site j. In the two-centre approximation, $\beta_{ij}^{\lambda\lambda'}$ can be expressed as a function of the direction cosines of the vector R_{ij} joining the two atoms i and j and of the four (ssσ), (spσ), (ppσ) and (ppπ) Slater–Koster (SK) parameters at the distance R_{ij} [22].

We must now fix the law of variation of hopping integrals with distance. One of the most used tight-binding Hamiltonians for silicon is the nearest-neighbour Hamiltonian of Chadi [2]. Following Harrison [23], Chadi assumed that all hopping integrals scale with the inverse square of the bond length R_{ij}. Several expressions of the nearest-neighbour repulsive term, E_{rep}, have been proposed in conjunction with this Hamiltonian. Chadi [2] used an expansion up to second order in the fractional change in bond length $\Delta R_{ij}/R_{ij}$, while, for instance, Harrison assumed an $(R_{ij})^{-4}$ dependence of the pair repulsion between atoms i and j.

However, these schemes have some drawbacks. First, the bulk band structure is not well reproduced when compared to *ab initio* calculations and, in particular, the width of the fundamental gap is overestimated. Moreover, when the $(R_{ij})^{-4}$ law is chosen for E_{rep}, the calculated bulk modulus (4.23 eV/atom) is only one-third of its experimental value (12.3 eV/atom) [24]. Finally, when surface reconstruction is investigated, the atomic displacements may be such that two atoms that were initially second-nearest neighbours become first-nearest neighbours or vice versa. This introduces a sizable discontinuity in the total energy, which can be reduced by extending the range of interaction to second-nearest neighbours. Furthermore, as shown by Pandey and Phillips [21], the introduction of second-nearest-neighbour hopping integrals leads to a significant improvement in the description of the valence band and of the bottom of the conduction band, which is the energy range of interest in total energy calculations and in the determination of surface state dispersion curves.

Table 1. Values of the different interatomic Slater–Koster parameters in the model of Pandey and Phillips [21].

Interactions	ssσ	spσ	ppσ	ppπ
First-nearest-neighbour value (eV)	−2.08	2.12	2.32	−0.52
Second-nearest-neighbour value (eV)	0.	0.	0.58	−0.10

Consequently, we will adopt, in this work, the second-nearest-neighbour tight-binding Hamiltonian of Pandey and Phillips for the equilibrium distances (see table 1). It is obvious from this table that the four types of parameters do not obey the same law of variation with distance. We first tried to use simple power or exponential laws, but, owing to the vanishing values of (ssσ) and (spσ) at the second-nearest-neighbour distance, these hopping integrals must rapidly decrease when the interatomic distance increases. This yields a huge value of the bulk modulus. Following Sawada [24], we solved this problem by using the product of a power law by an attenuation function, which may be different for each type of SK parameter, i.e.

$$\beta_{SK}^{\alpha}(R_{ij}) = \beta_{SK}^{\alpha}(R_0)[S_\alpha(R_{ij})/S_\alpha(R_0)](R_0/R_{ij})^{\nu_\alpha} \qquad (2)$$

with $\alpha = (ss\sigma)$, $(sp\sigma)$, $(pp\sigma)$, $(pp\pi)$ and where R_0 is the bulk equilibrium first-nearest-neighbour distance. The attenuation function S_α is given by

$$S_\alpha(r) = 1/\{1 + \exp[\mu_\alpha(r - R_\alpha)]\}. \tag{3}$$

The choice of the different electronic parameters is summarized in table 2. The first-nearest-neighbour SK parameters, and the atomic levels, E_s (taken as reference energy) and E_p (4.39 eV), are the same as in the model of Pandey and Phillips [21]. All ν_α and μ_α values are taken from Sawada's work [24]. If the R_α values given in this last work are used, the $(ss\sigma)$ and $(sp\sigma)$ at the second-nearest-neighbour distance are very small, in accordance with the values given by [21]. Conversely, the values of $(pp\sigma)$ and $(pp\pi)$ at this distance are significantly different from those of Pandey and Phillips [21] and, in particular, lead to a gap that is too wide. Hence, we slightly modified the corresponding R_α values in order to get the same dispersion curves as Pandey.

Table 2. Values of the parameters associated with the laws of variation of Slater–Koster parameters with interatomic distance.

α	$ss\sigma$	$sp\sigma$	$pp\sigma$	$pp\pi$
First-nearest-neighbour value (eV)	−2.08	2.12	2.32	−0.52
ν_α	4	3	2	2
R_α (Å)	3.17	3.17	4.05	3.77
μ_α (Å^{-1})	5.96	5.96	2.55	2.55

In our work, the repulsive energy is assumed to have the following form:

$$E_{rep}(R_{ij}) = A\sum_{i<j}\left(\frac{R_0}{R_{ij}}\right)^\eta. \tag{4}$$

The two constants A and η are fitted to give the experimental values of the first-nearest-neighbour distance and of the cohesive energy. In the bulk, the repulsive energy per atom in a diamond cubic lattice can be written as a function of the first-nearest-neighbour distance R:

$$E_{rep}(R) = 2A(R_0/R)^\eta\left[1 + 3\left(\tfrac{3}{8}\right)^{\eta/2}\right]. \tag{5}$$

The band contribution is given by

$$E_{band}(R) = 8\int^{E_F} En(E)\,dE - 2(E_s + E_p) \tag{6}$$

where $n(E)$ and E_F are, respectively, the electronic density of states and the Fermi level calculated for the first-nearest-neighbour distance R. The cohesive energy per atom is

$$E_{coh}(R) = E_{rep}(R) + E_{band}(R). \tag{7}$$

The parameters A and η are determined from the two conditions:

$$E_{\text{coh}}(R_0) = 4.6 \text{ eV} \qquad \text{and} \qquad (\mathrm{d}E_{\text{coh}}/\mathrm{d}R)_{R=R_0} = 0. \tag{8}$$

Once A and η are fixed, we can calculate the bulk modulus K given by

$$K = (R_0^2/9)\left(\mathrm{d}^2 E_{\text{band}}/\mathrm{d}R^2\right)_{R=R_0} + E_{\text{rep}}(R_0)(\eta(\eta+1)/9). \tag{9}$$

The calculation of E_{band} in the neighbourhood of $R = R_0$ needs a summation over the three-dimensional (3D) Brillouin zone. This is performed using the special-point technique [25] with 60 special points. We find

$$A = 3.34\,\text{eV} \qquad \eta = 5.48.$$

With these values of the repulsive potential parameters we obtain a bulk modulus (12.18 eV/atom) much closer to the experimental value (12.3 eV/atom) than that obtained by Sawada (10.53 eV/atom) and with Harrison's repulsive potential (4.23 eV/atom) [23, 24].

3. Tight-binding study of Si(100) surface

3.1. Tight-binding formalism for surfaces

It is usually assumed that, at the surface, the laws of variation of hopping integrals with distance are the same as in the bulk. However, the presence of the surface induces a charge rearrangement and, thus, a perturbation of the potential, which is taken into account by a shift, δV_λ^i, of the atomic levels of orbital λ at each site i. These shifts are obviously the same for each equivalent site. In our calculation, we consider that $\delta V_s^i = \delta V_p^i = \delta V_i$ as in the work of Priester *et al* [26].

The surface electronic band structure has been calculated using the slab method, which we will briefly summarize. The crystal is approximated by a finite number of layers parallel to the considered surface. Owing to the two-dimensional (2D) periodicity of the slab, the eigenstates associated with energy E_n and surface wavevector $q_{\|}$ can be written as

$$|n, q_{\|}\rangle = \sum_{m,j,\lambda} b_\lambda^j(E_n, q_{\|}) \exp(\mathrm{i} q_{\|} \cdot R_m) |m, j, \lambda\rangle. \tag{10}$$

Here R_m is the position vector of the unit cell m of the slab, and $|m, j, \lambda\rangle$ are the atomic orbitals centred on the jth inequivalent atom of the slab unit cell m. The partial local density of states associated with orbital λ of atom j, at a given $q_{\|}$, is defined by

$$n_{j,\lambda}(E, q_{\|}) = \sum_n b_\lambda^j(E_n, q_{\|}) b_\lambda^{j*}(E_n, q_{\|}) \delta(E_n - E). \tag{11}$$

Averaging over the surface Brillouin zone and over the different orbitals yields the local density of states (LDOS), $n_j(E)$, on atom j, normalized to unity. The change

in the number of electrons, δN_j, on atom j is directly related to the LDOS on atom j by

$$\delta N_j = 8 \int^{E_F} n_j(E, \ldots, \delta V_i, \ldots)\, \mathrm{d}E - 4. \tag{12}$$

When the surface is created, the variation of band energy, δE_{band}, can be obtained from the change, δn_j, of LDOS on each atom j by the formula

$$\delta E_{\text{band}} = \sum_j \left(8 \int^{E_F} E \delta n_j(E)\, \mathrm{d}E - 4\delta V_j - \tfrac{1}{2}\delta N_j \delta V_j \right). \tag{13}$$

The first term is the variation of the sum of one-electron energies and the last two terms arise from the double counting of the average Coulomb interaction between electrons in the first term. We must now turn to the calculation of δV_j. It is clear from (12) that the δN_j are a function of all δV_i. Reciprocally, the modification of the potentials, δV_j, is related to the charges on the different atoms through the Poisson equation. Ideally, the problem should be solved self-consistently. In transition metals, it has been shown that self-consistency considerably reduces the involved charges, and thus the shifts of atomic levels, which would be found in a completely self-consistent calculation, are close to the values that ensure the charge neutrality of each atom. This results from the quasi-perfect screening in metals. In silicon, the dielectric constant is so large that the screening is nearly complete [27] and we expect the local charge neutrality condition to be nearly obeyed. This approximation has already been used with success in semiconductors by Priester *et al* [26]. Consequently, in this work, we will determine the surface-induced shifts of atomic levels by assuming that the number of valence sp electrons on each atom is the same as in the bulk, i.e. four. Note that we can also assume a given charge transfer between atoms and calculate the corresponding δV_i. Such a calculation will be done in order to check the sensitivity of the results to a charge transfer.

3.2. Application to the (2 × 1) reconstruction of Si(100)

If it is easily understood that the formation of dimers on Si(100) by a pairing of surface atoms substantially lowers the total energy by reducing the number of dangling bonds, the exact geometry of the dimers is still subject to discussion. Using the formalism described above, the geometry could, in principle, be determined from the minimization of the total energy with respect to all atomic displacements. However, this would lead to extremely lengthy calculations and simplifying assumptions must be made. In this work, we neglect the displacements of sublayer atoms and we assume that the projection on the surface plane of the dimer bond remains along the [1,1,0] direction relative to the cubic axes (i.e. there is no twisting of the dimer). Hence, with the system of coordinates chosen here (see figure 1), the displacement of surface atoms is in the Oxz plane. Consequently, we minimize the total energy with respect to the displacements (DX_1, DZ_1) and (DX_2, DZ_2) of the two atoms of the dimers. We have considered successively the ideal surface and the reconstructed surfaces, with symmetric dimers ($DX_1 = DX_2$, $DZ_1 = DZ_2$) and asymmetric dimers.

In practice, the summation over $q_{\parallel}$ that is needed in the computation of the LDOS and of the sum of the one-electron energies is carried out using the special-point

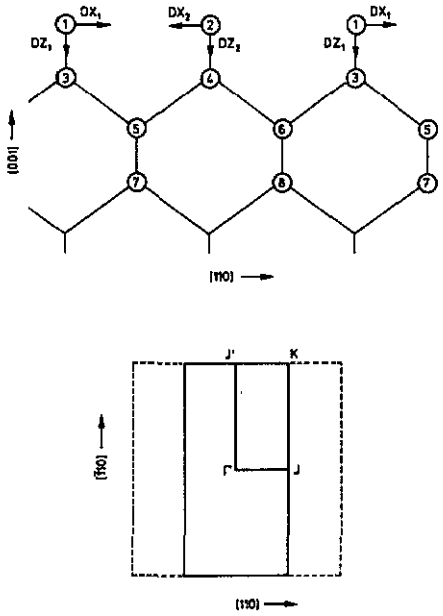

Figure 1. Side view of the (2 x 1) reconstruction of Si(100) and relevant surface Brillouin zone.

technique in the surface Brillouin zone [28]. We have checked the sensitivity of the results to the thickness of the slab and to the number of special points taken into account: when going from 16 to 64 special points in the irreducible part of the surface Brillouin zone or from a slab of 22 to 46 layers, the charge on each atom and the surface energy are modified at most by $2 \times 10^{-4} e^-$ and 10^{-3} eV per (2×1) unit cell, respectively. We have concluded that a sufficient accuracy is reached with 16 special points and a slab of 22 layers.

Even though the clean ideal surface has never been observed, it is of interest first to investigate this geometry to obtain the energy involved in the surface reconstruction. In order to compare accurately the different surface energies, we have used the (2×1) unit cell even for the ideal (1×1) surface. Neglecting the atomic level shifts, we obtain a surface energy of 3.57 eV per (2×1) unit cell. Using the local charge neutrality condition, this surface energy becomes 3.79 eV per (2×1) unit cell. The corresponding atomic level shifts of the surface and first three sublayer atoms are given in table 3.

Table 3. Atomic level shifts, in the ideal surface geometry, calculated using the local neutrality condition.

Layer number	Atomic level shift
1	0.78
2	0.38
3	0
4	0

The symmetric and asymmetric dimer configurations calculated by Ihm *et al* [1] have been used to start the minimization of the total energy for the reconstructed

surface. The determination of the configurations that minimize the energy has been carried out with and without the local charge neutrality condition in order to check the influence of the atomic level corrections.

Without correcting the atomic level shifts, two minima have been found, corresponding to symmetric and asymmetric dimer configurations, respectively. The atomic displacements associated with these geometries are given in table 4. The surface energies of these two configurations are $E_{sym} = 2.77$ eV and $E_{asym} = 2.74$ eV. Note that the energy difference between the two optimum geometries is very small (0.03 eV) compared to the reconstruction energy (0.8 eV/dimer) and is of the order of a phonon energy. Thus, if we neglect the atomic level corrections, we are led to the conclusion that the symmetric and asymmetric dimers would coexist at the surface at room temperature. This contrasts with the results of Chadi [2], Ihm *et al* [1] and Schmeits *et al* [29], which all strongly favour the asymmetric dimer, but is in agreement with a recent *ab initio* calculation of Shaoping Tang *et al* [30].

Table 4. Atomic displacements (Å) giving the two optimum geometries obtained when atomic level shifts are neglected.

Distortions	Symmetric dimer	Asymmetric dimer
DX_1	0.675	0.615
DX_2	0.675	0.806
DZ_1	0.184	0.069
DZ_2	0.184	0.380

The dimer bond lengths obtained in our calculations are 2.49 and 2.45 Å for the symmetric and asymmetric dimer, respectively. These values are significantly larger than the bulk bond length (2.35 Å), contrary to the results of other calculations. For example, the dimer bond length obtained by Batra [31] and Shaoping Tang *et al* [30] are in the range 2.22–2.27 Å. Our values are much closer to the experimental results, since, using low-energy ion scattering [6], it is found that the projection of the dimer bond length parallel to the surface is 2.4 ± 0.1 Å, and from LEED analyses the bond length is in the range $2.45 - 2.54$ Å [19, 20].

The dispersion curves relevant to symmetric and asymmetric equilibrium configurations are given in figures 2 and 3. The surface band structure for the asymmetric dimer is very similar to that obtained by Schmeits *et al* [29]. The corresponding LDOS on the dimer atoms is compared with the bulk DOS in figure 4. In the case of the symmetric dimer, the surface is metallic and the two surface state bands existing in the main gap give rise to two peaks in the LDOS. The lower surface state band, D^-, is located mainly just below the top of the valence band and the upper one, D^+, is in the absolute gap just above E_v. In the case of the asymmetric dimer, two surface state bands, D^- and D^+, are still found; however, D^- is almost completely localized on the up atom (atom 1) whereas D^+, although mainly localized on the down atom (atom 2), has a non-negligible weight on the up atom. The Fermi level E_F is located at the top of the valence band. However, the two asymmetric dimer atoms are heavily charged ($\delta N_1 = 0.7e^-$, $\delta N_2 = -0.5e^-$). As explained in the previous section, this means that self-consistency should be taken into account.

We have done the total energy minimization again but now correcting the atomic levels in such a way that each atom remains neutral.

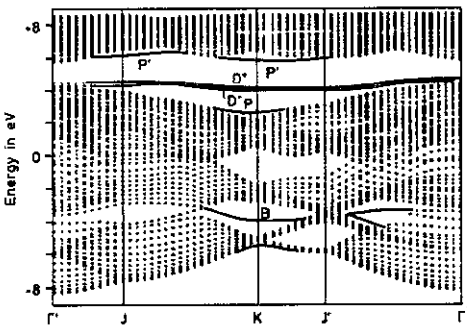

Figure 2. Surface band structure of Si(100) (2 × 1) for the equilibrium symmetric dimer geometry obtained when the atomic level shifts are neglected. The back-bond bands and the two dangling-bond states are labelled B, D^- and D^+, respectively. P and P′ are surface states having a p character.

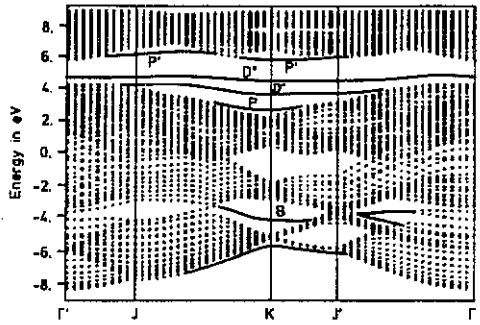

Figure 3. Surface band structure of Si(100) (2 × 1) for the equilibrium asymmetric dimer geometry obtained when the atomic level shifts are neglected. The back-bond bands and the two dangling-bond states are labelled B, D^- and D^+, respectively. P and P′ are surface states having a p character.

Table 5. Atomic displacements (Å) giving the optimum geometry obtained when the local neutrality condition is used.

Distortions	
DX_1	0.725
DX_2	0.725
DZ_1	0.218
DZ_2	0.218

In the symmetric geometry, we start the minimization from the same atomic configuration as previously. The minimum is found for atomic displacements given in table 5. The equilibrium dimer bond length is 2.39 Å, in good agreement with the above-mentioned experiments [6, 19, 20]. The corresponding shifts of atomic potential are given in table 6. Their relations with the surface core level shift measurement will be discussed in the next section. The surface and reconstruction energies per (2 × 1) unit cell are 2.8 and 1.0 eV, respectively. The dispersion curves and LDOS on the dimer atoms are given in figures 5 and 6. The surface state bands D^- and D^+ (figure 5) are very similar to those calculated with $\delta V_i = 0$. However, they are raised in energy by an amount of the order of the correction of the surface atomic levels. In figure 7, we see that they have a strong p_z character but also an s and a p_x contribution. This latter contribution is a consequence of the dimerization: the dangling bond that was pointing normal to the surface (its wavefunction was $(|s\rangle + |z\rangle)/\sqrt{2}$) is now tilted towards the Ox direction. Furthermore, these two surface state bands slightly overlap and the surface is metallic, the Fermi level being located in these bands. This result agrees with previous calculations on the symmetric dimer geometry but is in contradiction with what is commonly admitted on the basis of experimental results [32]. We will now discuss the two suggestions that have been put forward in order to open a gap in the surface state bands, i.e. either the tilt of the dimer, or an antiferromagnetic arrangement of the spins in the surface layer.

Assuming a charge neutrality of each atom, we have tried to start the energy mini-

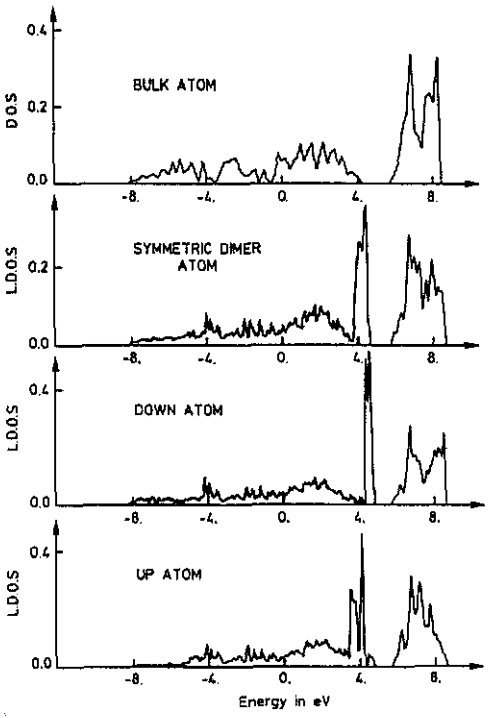

Figure 4. Comparison, with the bulk DOS, of the LDOS on the symmetric dimer atom and on the up and down atoms of the asymmetric dimer in the corresponding equilibrium geometries given in table 4 obtained when neglecting the atomic level shifts. (All the densities of states are normalized to unity.) The shaded areas correspond to the filled states. ($E_F = 4.25$ eV and 4.24 eV for the symmetric and asymmetric geometries, respectively.)

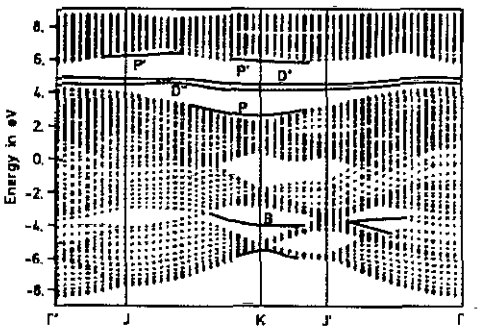

Figure 5. Surface band structure of Si(100) (2 × 1) for the equilibrium symmetric dimer geometry obtained in the local neutrality condition. The back-bond bands and the two dangling-bond states are labelled B, D^- and D^+, respectively. P and P′ are surface states having a p character.

mization from asymmetric configurations but, contrary to the non-self-consistent case, the minimizations have converged towards the same final symmetric configuration as that discussed just above. Thus, this suggests that a charge transfer between the up and down atoms of the dimer is necessary to stabilize an asymmetric configuration. We have checked that, on a given geometry, some energy is gained when charge is allowed to flow from the down atom to the up atom. The calculation has been carried out with the equilibrium asymmetric geometry obtained when neglecting the shifts of atomic levels. We have allowed a charge transfer of $0.3e^-$ from the down to the up atom while all sublayer atoms were assigned to be neutral. The surface energy, which is 3.08 eV per (2×1) unit cell, using the local charge neutrality is lowered to 2.95 eV when $0.3e^-$ is transferred. Obviously, the charge transfer should vary with the atomic displacements and vanish for the symmetric geometry. Ideally, for each geometry, a fully self-consistent calculation determining both δV_j and δN_i should be carried out as explained in section 3.1. However, the relation $\delta V_j = f(\delta N_i)$ introduces new parameters and approximations. Moreover, the calculations become

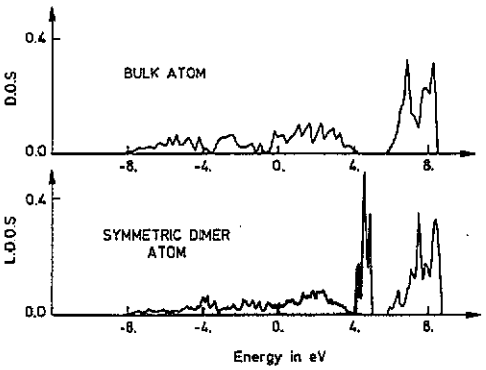

Figure 6. Comparison, with the bulk DOS, of the LDOS on the dimer atoms in the symmetric equilibrium geometry obtained in the local neutrality condition. (All the densities of states are normalized to unity.) The shaded area corresponds to the filled states ($E_F = 4.5$ eV).

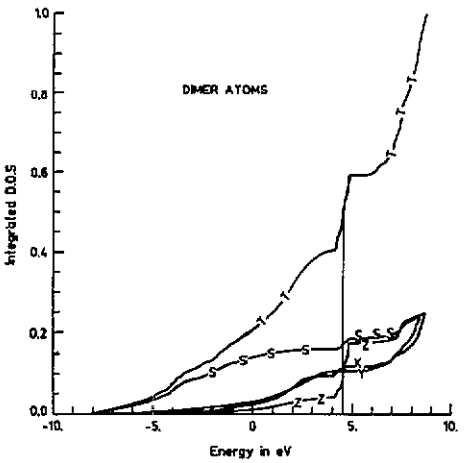

Figure 7. Total and partial integrated DOS on a dimer atom in the symmetric equilibrium geometry obtained in the local neutrality condition. (The total density has been normalized to unity.) Letters T, S, X, Y and Z denote, respectively, the total integrated density of states and the partial integrated densities of states associated with s, p_x, p_y and p_z orbitals.

Table 6. Atomic level shifts associated with the (symmetric) optimum geometry obtained in the local neutrality condition.

Atomic level shift (eV)	
δV_1	0.35
δV_2	0.35
δV_3	0.01
δV_4	0.01
δV_5	$\simeq 0$
δV_6	−0.14
δV_7	0
δV_8	0

quite lengthy and the final results may depend sensitively on parameters that are not accurately known. Nevertheless, as already stated, the charge transfer must be small in view of the large dielectric constant of silicon [27]. Indeed, since we have found that the stable geometry is a symmetric dimer for a zero charge transfer and as the self-consistent charge transfer should vary continuously as a function of the tilt of the dimer, we expect that, if a stable asymmetric configuration is found in a fully self-consistent calculation, the corresponding asymmetry must be small. In view of interpreting experimental surface core level shifts, some physical insight can be gained by comparing the values of the δV_i for the above asymmetric geometry and charge transfer with the values obtained for the equilibrium symmetric configuration. As a matter of fact, it can be inferred from all our calculations of atomic level shifts that the average value, δV_{av}, of δV_1 and δV_2 is always close to the value found for

the symmetric dimer while $(\delta V_1 - \delta V_{av})$ and $(\delta V_2 - \delta V_{av})$ increase in absolute value with the amplitude of the tilt but keep a constant sign. The results, assuming on the one hand a local charge neutrality and on the other hand a charge transfer of $0.3e^-$, are given in table 7. If we compare these results with those of table 6, we see that the effective atomic level on the up atom is shifted upwards in energy while that of the down atom is shifted downwards. Furthermore, for a given geometry, these effective atomic levels are not very sensitive to the assumed charge transfer. Finally, we note that δV_6 is negative and significant but almost insensitive to the geometry of the dimer and to the charge transfer, while δV_3, which is negligible for a symmetric dimer, becomes appreciable in the present asymmetric geometry.

Table 7. Comparison, at the optimum asymmetric geometry given in table 4, of the atomic level shifts obtained in the local neutrality condition or assuming a charge transfer of $0.3e^-$ from the down atom to the up atom.

Atomic level shift (eV)	Local neutrality on every atom	Charge transfer of $0.3e^-$ between up and down atoms
δV_1	0.72	0.64
δV_2	0.11	0.13
δV_3	0.30	0.28
δV_4	−0.10	−0.12
δV_5	0.00	0.00
δV_6	−0.17	−0.14
δV_7	0.00	0.00
δV_8	−0.10	−0.09

It is also of interest to compare the LDOS on the up and down atoms near the Fermi level. When the asymmetry is rather pronounced, we find that, above the Fermi level, the LDOS on both atoms are large whereas, below the Fermi level, the LDOS on the up atom is high and the LDOS on the down atom is low. Thus, if the surface is observed by scanning tunnelling spectroscopy, when empty states are studied, the dimers should appear roughly symmetric. Conversely, when investigating filled states, a buckling should be observed. Such an effect has been seen in experiments [10] but only near surface defects. Hence, far from these defects, the symmetric dimers observed on STM images can be viewed either as symmetric or as oscillating dimers. In this latter case it is expected that, the smaller the asymmetry, the easier the switching.

In conclusion, we think that a strong asymmetry of the dimers cannot exist on a perfect surface and we will see in the following section that this is corroborated by core level photoemission experiments. An asymmetry increases the separation between the two surface bands but, if this asymmetry is small, it cannot produce an absolute gap between them. In the symmetric dimer geometry, Artacho and Yndurain [5] have argued that an antiferromagnetic arrangement of the dimers lowers the total energy of the system and opens such a gap. However, this assertion is based on a Hartree–Fock approximation of a 2D lattice, thus neglecting the coupling with the sublayer atoms. In both approximations the tendency to find a magnetic solution is overestimated. Thus, it would be interesting to check that this result remains valid in a more elaborate calculation. The influence of a coupling of the surface plane with the bulk could be investigated using the same tight-binding Hamiltonian as above but adding a Hubbard term treated in the Hartree–Fock approximation, since it seems difficult, although not impossible, to go beyond this approximation. Moreover, to

clarify this issue completely, both spin effects and a slight asymmetry of the dimers should be considered. Even though we have some ideas as to how to improve matters, the topic is sufficiently complicated that we leave it for a future paper.

4. Comparison with surface core level photoemission experiments

It has been shown [33] that, in transition metals, the core levels of an atom experience a shift of the same sign and order of magnitude as the shift of its valence atomic level. Following the same argument, Priester *et al* [26] have been able to explain the observed core level shifts on the (110) surfaces of III–V semiconductors in the framework of the tight-binding approximation. As previously mentioned, they assumed that E_s and E_p experience the same shift and they calculated these shifts by ensuring local atomic charges equal to the bulk ones, i.e. local neutrality with respect to the bulk atoms. According to this point of view, the shifts δV_i given in tables 6 and 7 are directly comparable to surface core level shifts.

Let us now give a brief summary of experimental results of core level spectroscopy on Si(100). Before any deconvolution all spectra show a shoulder, on the low-binding-energy side of the bulk peak, which is clearly due to surface atoms since its intensity is, on the one hand, sensitive to surface pollution and, on the other hand, maximum at a photon energy for which the electron mean free path is at a minimum. Moreover, the valley between the spin–orbit split $2p_{1/2,3/2}$ doublet is less pronounced in surface than in bulk sensitive spectra.

These spectra have been interpreted in several ways. According to some authors [12–14], there is only one surface component above each bulk peak (i.e. at negative binding energy shift relative to bulk Si) possibly split by at most the energy resolution of the experiment ($\simeq$ 200 meV). Himpsel *et al* [15, 16] assign the pronounced surface core level shoulder above the bulk line to half a monolayer of outer dimer atoms. Furthermore, in their decomposition, they obtain other components, and in particular one below the bulk line. They assign these components to other perturbed atoms which, according to the intensities and their assumed escape depth of 5.4 Å, should belong to the outer two surface layers. The existence of at least one peak on each side of the bulk peak is corroborated by an experiment due to McGrath *et al* [17]. Finally, in a very recent experiment, Wertheim *et al* [18] interpret their data, after deconvolution of the spin–orbit doublet, with three surface components for each bulk peak. They assign to the up atom of an asymmetric dimer a doublet, split by $\simeq$ 190 meV owing to the crystal field, with an average shift of $\simeq$ 400 meV above the bulk peak. They ascribe to the down atom a line, below the bulk peak, for which they find a Doniach–Sunjic lineshape.

Let us now compare the experimental values of surface core level shifts with the set of values of δV_i given in tables 3, 6 and 7. In the symmetric dimer model, we expect that the spectrum of a given core level presents three peaks: the bulk peak B, a peak S_1 at 350 meV from B on its lower-binding-energy side associated with the dimer atoms and a peak S_2 at 140 meV from B on its higher-binding-energy side associated with atom 6 (see figure 1). The other peaks due to atoms 3, 4 and 5 are indistinguishable from the bulk peak. As mentioned above, a charge transfer is necessary to stabilize the asymmetric dimer. This charge transfer should vary with the atomic displacements and, thus, the determination of the equilibrium geometry would require a fully self-consistent calculation, which would be very lengthy. However, it is

possible to determine qualitatively from table 7 the evolution of the core level shifts when going from a symmetric to an asymmetric configuration. We see on this table that the main effect of an asymmetry is to split the line S_1 due to the dimer atoms into one component, S_1', at lower binding energy due to the up atom, and another component, S_1'', at higher binding energy due to the down atom. Conversely, the line S_2 due to atom 6 is rather insensitive to the asymmetry of the dimer. Moreover, the results do not vary very much with the charge transfer, even for a value as large as $0.3e^-$, which is probably overestimated. The comparison of these calculated results with experiments suggests that there exists an asymmetry that is weaker than that computed with $\delta V_i = 0$. Finally, the peaks associated with atoms 3 and 4, which would give rise to new lines if the asymmetry were large, are expected to remain close to the bulk peak in the case of a weak asymmetry. To summarize, we propose the following interpretation of the experimental data. The doublet S_1', S_1'' on the lower-binding-energy side of the bulk peak is attributed to the dimer atoms in a slightly asymmetric configuration. The line S_2 on the higher-binding-energy side of the bulk peak is assigned to atom 6. Note that the degree of asymmetry of the dimers may depend on the presence of defects such as steps, missing dimers, etc. Furthermore, according to this interpretation, the intensity of the lines S_1', S_1'' and S_2 should be roughly equal in an angle-integrated core level photoemission experiment since atom 6 has no neighbours in a wide solid angle above it. This is qualitatively verified on the spectrum given in figure 2 of Himpsel *et al* [16].

This interpretation of the origin of the different lines disagrees with that proposed by Wertheim *et al* [18] since these authors attribute the splitting between S_1' and S_1'' to a crystal-field effect. Such an effect can be expected when the populations of the three p orbitals on the considered atom differ significantly. According to our calculations, this is not the case for the symmetric dimer. In the asymmetric geometry, assuming a charge transfer of $0.3e^-$, we find that the population of the p_z orbital is significantly larger (smaller) than that of p_x or p_y on the up (down) atom, respectively. Consequently, if a crystal-field effect is expected, it should appear on both atoms of the dimer with the same order of magnitude. Moreover, Wertheim *et al* associate the peak S_2 to the down atom of the dimer from a lineshape argument: they find that their best fit to the experimental spectrum is obtained by giving this peak an asymmetric Doniach–Sunjic lineshape, which they explain by the presence of electronic excitations from the valence band into the nearby surface state. This can be understood if, on the one hand, the lower surface band is completely filled and totally localized on the up atom and, on the other hand, if the higher surface state band D^+ is completely empty and totally localized on the down atom. Moreover, the two surface state bands must be near the top of the valence band. If this latter condition is well verified in our calculations, the former ones are not; in particular, D^+ has a significant weight on the up atom and, thus, excitations of electron–hole pairs at very low energy are also possible on this atom. Consequently, the peaks associated with the up and down atoms may both have an asymmetric lineshape. However, if in our interpretation, this lineshape asymmetry could exist for the peak S_1' and S_1'', the peak S_2 should not have any asymmetry since, the weight on atom 6 of the surface state bands being very small, the density of states near the Fermi level is very low.

5. Conclusions

In this paper, we have defined a tight-binding model consistent with electronic band

structure as well as elastic properties of bulk silicon. With this model, we have investigated the different geometries of dimerized reconstruction of the Si(100) (2×1) surface. In all cases, the calculated bond lengths are in much better agreement with experiment than in previous calculations. If it is assumed that the atomic levels remain the same on surface atoms as on the bulk atoms, we find, as in most recent theoretical studies, that the difference in energy between the symmetric and asymmetric dimer reconstruction is small and must be of the order of a phonon energy. Since, in this approximation, the charges on some atoms are unrealistic, the atomic level shifts of surface atoms have been determined, in a second approach, from a local charge neutrality condition. In this case, the minimization of the total energy has always led to a symmetric configuration in which the surface is metallic. However, core level experiments cannot be explained without some asymmetry of the dimers. This result does not seem in contradiction with our model if a small charge transfer between the dimer atoms is allowed. Nevertheless, the asymmetry should be weak for several reasons. First, a rather large asymmetry would produce a charge transfer between the dimer atoms, the magnitude of which seems inconsistent with the large value of the dielectric constant of silicon. Then, according to our interpretation of core level photoemission data, the splitting between the surface core levels observed at lower binding energy with respect to the bulk core level is attributed to the tilt of the dimer and is rather small. However, such a tilt is not sufficient to produce an absolute gap between the two surface state bands as seen in UPS experiments, and magnetic effects should be invoked. Further calculations including these effects would be very interesting.

References

[1] Ihm J, Cohen M L and Chadi D J 1980 *Phys. Rev.* B **21** 4592
[2] Chadi D J 1979 *Phys. Rev. Lett.* **43** 43; 1979 *J. Vac. Sci. Technol.* **16** 1290
[3] Wolfgarten G, Kruger P and Pollmann J 1985 *Solid State Commun.* **54** 839
[4] Pandey K C 1985 *Proc. 17th Int. Conf. on the Physics of Semiconductors (San Francisco, 1984)* ed D J Chadi and W A Harrison (Berlin: Springer) p 55
[5] Artacho E and Yndurain F 1989 *Phys. Rev. Lett.* **62** 2491
[6] Aono M, Hou Y, Oshima C and Ishizawa Y 1982 *Phys. Rev. Lett.* **49** 567
[7] Hamers R J, Tromp R M and Demuth J E 1986 *Phys. Rev.* B **34** 5343
[8] Tromp R M, Hamers R J and Demuth J E 1985 *Phys. Rev. Lett.* **55** 1303
[9] Hamers R J, Tromp R M and Demuth J E 1987 *Surf. Sci.* **181** 346
[10] Kochansky G P and Griffith J 1991 *Surf. Sci. Lett.* **249** L293
[11] Johansson L S O, Uhrberg R I G, Martensson P and Hansson G V 1990 *Phys. Rev.* B **42** 1305
[12] Rich D H, Miller T and Chiang T C 1988 *Phys. Rev.* B **37** 3124
[13] Larsson C U S, Flodstrom A S, Nyholm R, Incoccia L and Senf F 1987 *J. Vac. Sci. Technol.* A **5** 332
[14] Bringans R D, Olmstead M A, Uhrberg R I G and Bachrach R Z 1987 *Phys. Rev.* B **36** 9569
[15] Himpsel F J, McFeely F R, Taleb-Ibrahimi A, Yarmoff J A and Hollinger G 1988 *Phys. Rev.* B **38** 6084
[16] Himpsel F J, Heinmann P, Chiang T C and Eastman D E 1980 *Phys. Rev. Lett.* **45** 1112
[17] McGrath R, Cimino R, Braun W, Thornton G and McGovern I T 1988 *Vacuum* **38** 251
[18] Wertheim G K, Riffe D M, Rowe J E and Citrin P H 1991 *Phys. Rev. Lett.* **67** 120
[19] Tong S Y and Maldonado A L 1978 *Surf. Sci.* **78** 459
[20] Yang W S, Jona F and Marcus P M 1983 *Phys. Rev.* B **28** 2049
[21] Pandey K C and Phillips J C 1974 *Phys. Rev. Lett.* **32** 1433; 1976 *Phys. Rev.* B **13** 750
[22] Slater J C and Koster G F 1954 *Phys. Rev.* **94** 1498
[23] Harrison W A 1980 *Electronic Structure and the Properties of Solids* (San Francisco: Freeman)
[24] Sawada S 1990 *Vacuum* **41** 612

[25] Chadi D J and Cohen M L 1973 *Phys. Rev.* B **8** 5747
[26] Priester C, Allan G and Lannoo M 1987 *Phys. Rev. Lett.* **58** 1989
[27] Himpsel F J, Meyerson B S, McFeely F R, Morar J F, Taleb-Ibrahimi A and Yarmoff J A 1990 *Photoemission and Adsorption Spectroscopy of Solids and Interfaces with Synchrotron Radiation (Enrico Fermi School, Varenna)* ed M Campagna and R Rosei (Amsterdam: North-Holland) p 203
[28] Cunningham S L 1974 *Phys. Rev.* B **10** 4988
[29] Schmeits M, Mazur A and Pollmann J 1983 *Phys. Rev.* B **27** 5012
[30] Shaoping Tang, Freeman A J and Delley B 1992 *Phys. Rev.* B **45** 1776
[31] Batra I P 1990 *Phys. Rev.* B **41** 5048
[32] Himpsel F J and Eastman D E 1979 *J. Vac. Sci. Technol.* **16** 1920
[33] Spanjaard D, Guillot C, Desjonquères M C, Tréglia G and Lecante J 1985 *Surf. Sci. Rep.* **5** 1